1×5 reconfigurable optical wireless routers for on-chip interconnection

Loredana Gabriele[1], Gaetano Bellanca[2*], Jacopo Nanni[3], Marina Barbiroli[3], Franco Fuschini[3], Velio Tralli[2], Davide Bertozzi[2], Giovanni Serafino[4], Vincenzo Petruzzelli[1], and Giovanna Calò[1]

[1]Department of Electrical and Information Engineering, Polytechnic University of Bari, Via Orabona, 4, Bari 70125, Italy
[2]Department of Engineering, University of Ferrara, Via Saragat, 1, Ferrara 44122, Italy
[3]Department of Electrical, Electronic and Information Engineering "G. Marconi", University of Bologna, Viale del Risorgimento, 2, Bologna 40136, Italy
[4]Scuola Superiore Sant'Anna, TeCIP Institute, via G. Moruzzi 1, 56124 Pisa, Italy
[*] gaetano.bellanca@unife.it

In this paper we report the design of 1×5 wireless routers, based on transmitting and receiving integrated Optical Phased Arrays (OPA), which allow on-chip optical wireless interconnections. The proposed devices aim at achieving high-bandwidth and reconfigurable links between multiple nodes. The general design criteria of these routers are reported and performance increase in terms of insertion loss and crosstalk, obtained by increasing the number of antennas in each OPA, are demonstrated.
Keywords: *wireless optical interconnects, optical antennas, optical phased arrays.*

INTRODUCTION

Chip Multiprocessors (CMPs) exploiting the potentialities of parallel computing are the state-of-the-art solution to face the constant need of increasing computing system efficiency. As the number of cores in chip multiprocessors continues to scale up, the efficient interconnection of these cores is becoming a major challenge to avoid communication bottleneck and to meet the high bandwidth, low-power and low-latency requirements which, actually, cannot be matched by traditional point-to-point connections through dedicated electrical links [1].
The realization of efficient on-chip interconnections is one of the most important challenges in developing new computing architectures based on heterogeneous multichip integration. In order to overcome the communication bottleneck of these multichip systems, in this work we propose a new approach based on the use of optical wireless routers. These routers can be integrated with an existing Optical Network on Chip as an alternative to ring-based routing matrices, with the aim to increase the overall efficiency of the network. Different configurations of on-chip 1×5 optical wireless interconnections are proposed. These configurations exploit transmitting and receiving Optical Phased Arrays (OPAs) made of taper antennas [2, 3]. We report the wireless router design criteria as well as the results of three-dimensional Finite Difference Time Domain (FDTD) simulations. The effect of the multipath propagation in the on-chip multi-layered medium is also taken into account.

RESULTS

A conceptual scheme of a 1×5 Optical Wireless Interconnection Block (OWIB) is shown in Fig. 1 (a), while the cross section of the on-chip multilayer structure is illustrated in Fig. 1 (b) [4]. In this scenario, the transmitting OPA can illuminate five different receivers, provided that suitable phase shifts are applied at the different antennas in each OPA. The phase shift of the optical signal applied at the input of the different antennas, allows tilting the radiated beam toward the selected receiving OPA. To guarantee the interconnection between the transmitter and the addressed receiver, a suitable phase shift must be applied also at the receiving OPA, to virtually steer the radiation diagram of the receiving array.

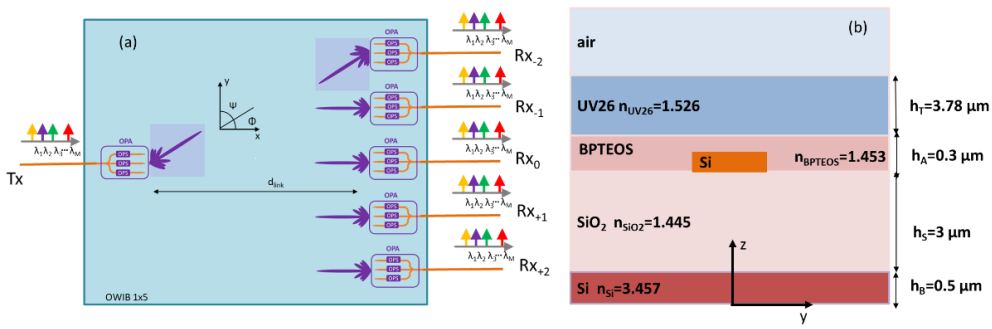

Fig. 1. (a) Scheme of a 1×5 OWIB. OPA: Optical Phase Array; OPS: Optical Phase-Shifter; (b) On-chip multilayer structure (yz-cross section), highlighting the multiple interfaces in the vertical plane.

The phase shift necessary for the OWIB operation can be achieved in Si waveguides by using Optical Phase Shifters (OPSs) based either on thermo-optic or plasma-optic effect [5]. In the scheme of Fig. 1 (a), the antennas are integrated with standard waveguides and they radiate a wavelength-division multiplexed (WDM) signal with parallel and simultaneous transmission of different data channels. The wireless propagation of the optical signal occurs in the on-chip multilayered structure shown in Fig. 2 (b), which was already analyzed by the authors in [3, 4, 6].

The transmitting and receiving OPAs schematized in Fig. 1 (a) are made by aligning some antennas along the y-axis; each antenna is made by inversely tapering a standard SOI waveguide, with cross-section height h = 220 nm and width w = 450 nm. The taper, having length L_T = 2 µm, is terminated on a small tip with length l = 1 µm, and width w_T = 130 nm. The guided mode becomes evanescent while propagating in the inverse taper and, therefore, it is radiated in the surrounding dielectric.

Two different 1×5 OWIB configurations are analyzed, namely: 1) a 1×5 OWIB exploiting N = 3 antennas for each OPA with distance $d_a = 2\lambda/n_{UV26}$ (where λ/n_{UV26} is the wavelength in the cladding medium) between adjacent antennas, and 2) a 1×5 OWIB exploiting N = 5 antennas for each OPA, having one half of the distance ($d_a = \lambda/n_{UV26}$) between the adjacent elements.

Figs. 2 show the calculated radiation diagrams of the two analyzed OPA configurations as a function of the angle Φ on the horizontal plane with (a) N = 3 and (b) N = 5 antennas, for different applied phase shifts. The radiation diagram of the single taper antenna is also reported in Figs. 2 (black curve), for the sake of comparison. To calculate the radiation diagrams, the antenna arrays were modeled through the FDTD method. Standard near-to-far field projections of the fields recorded on a closed box, surrounding the antenna and the SOI waveguides, were calculated after the Fourier transformation of the time-domain electromagnetic fields [3, 7]. As can be seen in Figs. 2, both configurations allow addressing 5 receivers. In the first configuration (Fig. 2 (a)), the distance between the N = 3 antennas is $d_a = 2\lambda/n_{UV26}$. As expected from antenna theory, distances d_a between adjacent radiators greater than the wavelength in the propagation medium, lead to having multiple main lobes in the visible space. This feature can be exploited in the design of the OPA to address multiple receivers.

As an example, when a phase shift equal to α = ±360°/N = ±120° is applied to the array elements of the transmitter, it is possible to steer the maxima of the radiation diagram to the positions of the radiation nulls of the broadside array (α = 0, yellow curve). In this way, either $Rx_{\pm1}$ or $Rx_{\pm2}$ can be illuminated. To minimize crosstalk, the five receivers Rx_i (with i = 0, ±1, ±2) should be placed in correspondence of the radiation peaks/nulls.

In the second configuration (Fig. 2 (b)), the distance between the N = 5 antennas is halved ($d_a = \lambda/n_{UV26}$). In this case, the antenna gain exhibits a single main lobe for every phase shift considered. When the phase shifts α = ±360°/N = ±72° and α = ±2·360°/N = ±144° are applied to the array elements of the transmitter, it is possible to steer the maxima of the radiation diagram to the positions of the radiation nulls of the broadside array (α = 0, yellow curve).

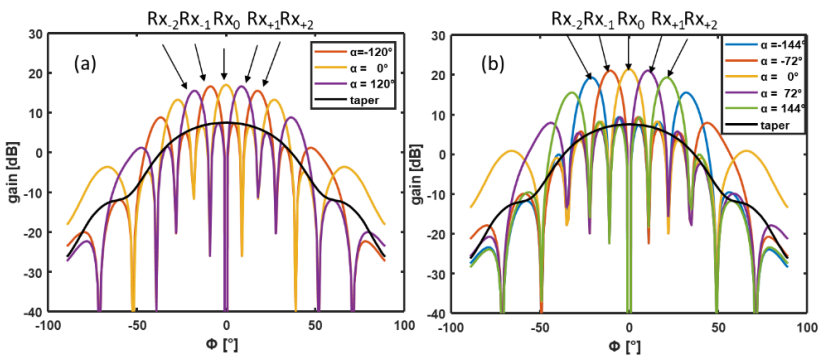

Fig. 2. Gain as a function of the angle Φ for different values of the phase shift α calculated for: (a) an array of N = 3 taper antennas with antenna distance $d = 2\lambda/n_{UV26}$, and (b) an array of N = 5 taper antennas with antenna distance $d = \lambda/n_{UV26}$. The taper length is L_T = 2 µm and the gain of the taper antenna is also reported (black curve). The wavelength is 1550 nm.

In order to evaluate the performances of the two OWIB configurations, the full devices (made of 1 transmitting and 5 receiving OPAs) were simulated by FDTD considering the propagation in the multilayered medium schematized in Fig. 1 (b). The transmittances of every link, computed as the total power coupled into the receiver waveguides divided by that at the transmitter, were calculated for the different phase-shift values. In both configurations, the distance d_{link} between the transmitters and the receivers, and the distance between the different receiving OPAs, were optimized to minimize crosstalk and multi-path attenuation [4].

Figs. 3 show the transmittance in dB, calculated as a function of the wavelength, at the receiving OPAs, i.e. Rx_0, $Rx_{\pm1}$ and $Rx_{\pm2}$, with three taper antennas for each array; the taper length is L_T = 2 µm, the antenna distance is $d = 2\lambda/n_{UV26}$ and the link distance is d_{link} = 55 µm. The receivers (a) Rx_0, (b) Rx_{+1}, and (c) Rx_{+2} are addressed by applying the indicated phase shifts at the transmitting and at the receiving OPAs. The transmittances pertaining to the links

between the transmitter and either Rx_{-1} and Rx_{-2} are not reported since, for the symmetry of the device, they are similar to Figs. 3 (b) and (c).

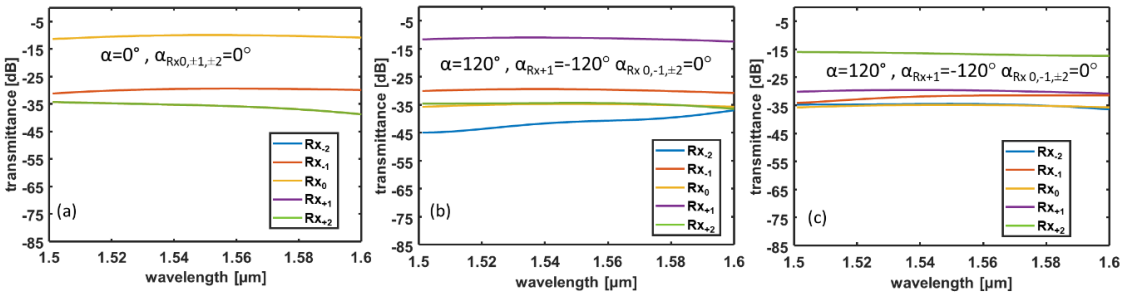

Fig. 3: Transmittance (in dB), calculated as a function of the wavelength, at the receiving OPAs, i.e. Rx_0, $Rx_{\pm1}$ and $Rx_{\pm2}$, with three taper antennas for each array (taper length L_T = 2 μm, antenna distance d = 2λ/n_{UV26} and link distance d_{link} = 55 μm). The receivers (a) Rx_0, (b) Rx_{+1}, and (c) Rx_{+2} are addressed by applying the indicated phase shifts at the Tx and at the Rx OPAs.

Similarly, Figs. 4 show the performances at the receiving OPAs, i.e. Rx_0, $Rx_{\pm1}$ and $Rx_{\pm2}$, with five taper antennas for each array. In this case, the taper length is L_T = 2 μm, the antenna distance is d = λ/n_{UV26}, and the link distance is d_{link} = 65 μm. As before, the receivers (a) Rx_0, (b) Rx_{+1}, and (c) Rx_{+2} are addressed by applying the indicated phase shifts at the transmitting and at the receiving OPAs.

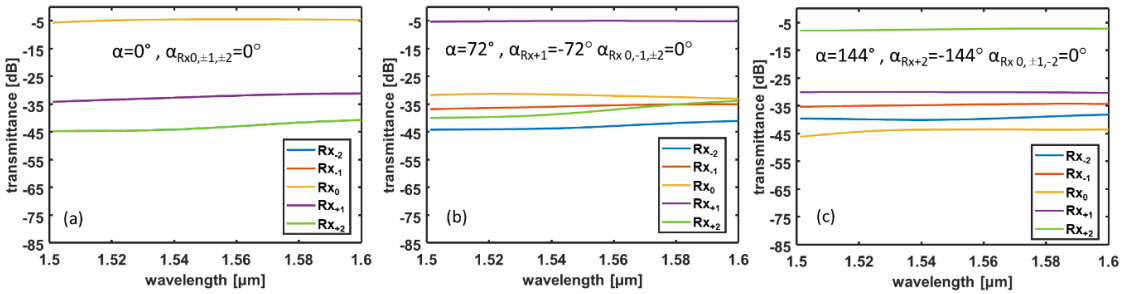

Fig. 4: Transmittance (in dB), calculated as a function of the wavelength, at the receiving OPAs, i.e. Rx_0, $Rx_{\pm1}$ and $Rx_{\pm2}$, with five taper antennas for each array (taper length L_T = 2 μm, antenna distance d = λ/n_{UV26}, and link distance d_{link} = 65 μm). The receivers (a) Rx_0, (b) Rx_{+1}, and (c) Rx_{+2} are addressed by applying the indicated phase shifts at the Tx and at the Rx OPAs.

DISCUSSION

From Figs. 3 we can infer that, for the OWIB exploiting OPAs with N = 3 antennas, the worst-case insertion loss IL ≈ -15 dB occurs when the receivers $Rx_{\pm2}$ are addressed. Moreover, the crosstalk between the different ports can be determined as $XT_{ij} = 10\ Log_{10}(T_{Rxi}/T_{Rxj})$, where T_{Rxj} is the transmittance of the addressed port and T_{Rxi} is the transmittance of a non-addressed one. For the OWIB exploiting OPAs with N = 3 antennas, the worst-case crosstalk XT_{21} ≈ -12 dB occurs for the links Tx→Rx_{+2} and between the nodes Rx_{+1} and Rx_{+2}. Similarly, from Figs. 4 we can observe that, for the OWIB exploiting OPAs with N = 5 antennas, the worst-case insertion loss occurs, again, when the receivers Rx_{+2} is addressed. However, thanks to the higher gain of the OPA, the worst-case insertion loss is lower IL ≈ -7.5 dB. Also, the crosstalk is improved with a worst-case value XT_{21} ≈ -22 dB for the link Tx→Rx_{+2} and between the receivers Rx_{+1} and Rx_{+2}. Therefore, increasing the number of antennas in the OPA improves the OWIB performances. As a counterpart, this increases device footprint and complexity of the phase-shifting circuitry.

References

[1] J. Flich and D. Bertozzi, Designing Network-on-Chip Architectures in the Nanoscale Era (CRC Press, 2019).

[2] C. García-Meca, et Al., "On-chip wireless silicon photonics: from reconfigurable interconnects to lab-on-chip devices," Light Sci Appl 6(9), e17053 (2017).

[3] G. Calò, et Al., "Design of reconfigurable on-chip wireless interconnections through optical phased arrays," Optics Express, vol. 29, no. 20, pp. 31 212–31 228, 2021.

[4] J. Nanni et al., "Multi-path propagation in on-chip optical wireless links," IEEE Photonics Technology Letters, vol. 32, no. 17, pp. 1101–1104, 2020.

[5] W.N. Ye and Y. Xiong, "Review of silicon photonics: history and recent advances," J. Mod. Opt. 60(16), 1299–1320, (2013).

[6] B. Alam, et al., "Numerical and experimental analysis of on-chip optical wireless links in presence of obstacles," IEEE Photonics Journal, vol. 13, no. 1, pp. 1–11, 2020.

[7] G. Calò et al., "Double Vivaldi antenna for wireless optical networks on chip", Optical and Quantum Electronics, Vol. 50, n. 6, Article number 261, 2018